International Journal of Nanoelectronics and Materials
Volume 15 (Special Issue) December 2022 [341-349]

A Comparative Investigation on Liquid-Based Memristor Sensor for Glucose Detection

Bibi Nadia Taib[1,2], Asrulnizam Abd Manaf[1], and Norhayati Sabani[2]

[1]Collaborative Microelectronic Design Excellence Centre (CEDEC), Universiti Sains Malaysia, Penang, Malaysia
[2]Faculty of Electronic Engineering Technology, Universiti Malaysia Perlis, Perlis, Malaysia

ABSTRACT

This study reports a comparison of the behavior of liquid-based memristor sensors when tested with different concentrations of liquid glucose. A thin film of titanium dioxide (TiO_2) serves as the sensing layer and is prepared through a sol-gel process using a spin coating method. This TiO_2 layer has been spin coated on three sensors with a spin speed of 2000, 2500 and 3000 rpm respectively. A nine-well structure was patterned on the TiO_2 layer for all three sensors. Four different concentrations of liquid D-glucose 10, 20, 30, and 40 mM were tested on this sensor. These memristor sensors were characterized using a Keithley 4200-SCS Semiconductor Characterization System for current-voltage (I-V) measurements. The experimental results show that the R_{OFF}/R_{ON} (off-state resistance to on-state resistance ratio) increases as the glucose concentration increases in line with the increase in the spin speed of TiO_2 sol-gel coating. The memristor sensor with the highest glucose concentration at the highest spin speed of 3000 rpm resulted in the highest R_{OFF}/R_{ON} ratio of 2.25 and subsequently contributed to the highest sensitivity of 56.25 $(mM)^{-1}$. In conclusion, increasing the spin speed of the TiO_2 sol-gel coating will increase the ratio and thus increase the sensitivity of the sensor.

Keywords: Liquid-based memristor sensor; R_{OFF}/R_{ON} ratio; sol-gel spin coating

1. INTRODUCTION

The memristor was theoretically introduced as the fourth fundamental circuit element by Leon O. Chua in 1971 [1]. Memristor behavior is presented by a pinched hysteresis loop in two constitutive variables, current-voltage (I-V) [2]. In 2008, scientists at Hewlett Packard's lab succeeded in fabricating the first practical memristor device [3]. To date, numerous application areas have been explored by scientists to ascertain the potential areas for memristor applications.

The largest memristor research is in memory applications. This is because memristors have the advantage of being non-volatile (retaining memory without power). In addition, there are other potential areas of investigation namely computing, neuromorphic [4], and sensing [5-8]. Memristor behavior is represented mathematically by the R_{OFF}/R_{ON} ratio [9-10]. This ratio is available at different reading voltages. A good memory device has a high R_{OFF}/R_{ON} ratio and vice versa.

The R_{OFF}/R_{ON} ratio is not only used in memory applications, but is also used in sensing applications to determine the sensing capability of memristor devices. This ratio is represented by the hysteresis loop area of the memristor. In sensing applications, a high R_{OFF}/R_{ON} ratio will result in a high sensitivity sensor. The behavior of the memristor biosensor is examined by the voltage gap between the minimum current reached in the forward and backward branches of the I - V curve [5], [11–18].

* bibinadia@unimap.edu.my

In this study, a liquid-based memristor sensor with a nine-well structure on a TiO_2 layer is designed and fabricated to detect four different concentrations of liquid D-glucose of 10, 20, 30, and 40 mM. The function of the well structure is to allow a chemical reaction between liquid and sensing layer. A memristor sensor structure consisting of a thin layer of TiO_2 is expected to create a chemical reaction with liquid D-glucose, $C_6H_{12}O_6$. The hydroxide ion, OH^- from glucose will react with oxide ion, O^{2-} at TiO_2 thin film surface and produce different behavior of memristor for different glucose concentration.

The behavior of this sensor will be analyzed in terms of the hysteresis loop area determined by the R_{OFF}/R_{ON} ratio. The values of R_{ON} and R_{OFF} are obtained using the equation (1) and (2). The ratio will change when detecting a specific liquid because it depends on the composition and concentration of the liquid. Changes in this ratio will affect the sensitivity of the sensor. The sensitivity, S of a liquid-based memristor sensor can be calculated using equation (3).

$$R_{ON} = \frac{Reading\ Voltage}{I_{ON}} \tag{1}$$

$$R_{OFF} = \frac{Reading\ Voltage}{I_{OFF}} \tag{2}$$

$$S = \frac{\frac{R_{OFF}}{R_{ON}} ratio}{D{-}glucose\ concentration} \tag{3}$$

Figure 1 shows the location of R_{ON} and R_{OFF} in the I-V characteristic. The R_{OFF}/R_{ON} ratio can be calculated on the loop area in a positive voltage sweep or the loop area in a negative voltage sweep. This study consider the switching behavior of the memristor as unipolar switching. In unipolar switching, the positive and negative voltage sweeps are at the same value where the memristor can be switched by applying voltages of the same or opposite polarity continuously. This means that the resistance value can change with the same pole voltage [19].

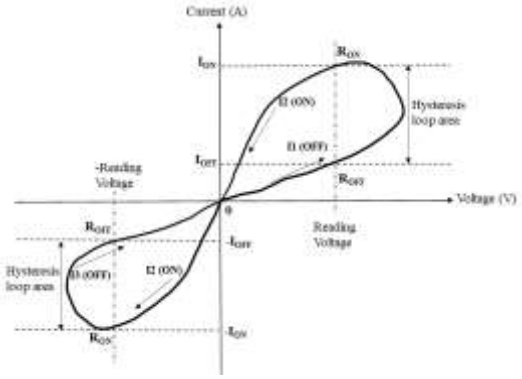

Figure 1. I-V characteristic of memristor [20].

2. METHODOLOGY

2.1 Mask Design

Before starting the fabrication process, the masks need to be designed using AutoCAD software. FIGURE 2 shows all three masks (top view) that involve in fabricating a liquid-based memristor sensor. The 1st & 2nd masks are printed on a metal plate while 3rd mask is printed on a plastic mold.

(a) 1st mask (b) 2nd mask (c) 3rd mask

Figure 2. Three masks were designed using AutoCAD (a) 1st mask (patterning the nine-well structure on the TiO_2 layer) (b) 2nd mask (patterning the Aluminum layer) and (c) 3rd mask (patterning the PDMS layer).

2.2 Fabrication

The fabrication process begins by cutting Indium Tin Oxide (ITO) coated glass to a size of 50 mm x 30 mm using a glass cutter. ITO glass is used as a substrate for memristor sensors. The entire fabrication processes for the memristor sensor are recorded in Table 1.

Table 1 Fabrication processes of liquid-based memristor sensor

Step No.	Process steps	Time
1	Cleaning of ITO glass using ethanol followed by acetone and also deionized water in an ultrasonic bath	30 minutes
2	Spray drying the ITO glass using nitrogen gas	3 minutes
3	Preparation of TiO_2 sol-gel solution:	
	(i) Mix and stir solution A (2.5 ml glacial acetic acid 99%, 1.5 ml titanium isopropoxide 97% and 23 ml absolute ethanol 99.8%) at a speed of 1500 rpm	1 ½ hour
	(ii) Mix and stir solution B (3 drops Triton X-100, 0.2 ml deionized water and 23 ml absolute ethanol 99.8%) at a speed of 1500 rpm	1 ½ hour
	(iii) Mix and stir solution A and solution B at a speed of 1500 rpm	1 ½ hour
4	Deposition of TiO_2 thin films on ITO glass using TiO_2 sol-gel spin coating method at three different spin speeds:	
	(i) 2000 rpm	25 seconds
	(ii) 2500 rpm	25 seconds
	(iii) 3000 rpm	25 seconds
5	Post-bake at 200°C in furnace	10 minutes
6	TiO_2 thin film etching using Reactive Ion Etch (RIE) machine with 1st mask (metal mask) to pattern nine-well structure with diameter of 3.0 mm	45 seconds
7	Aluminum (Al) deposition on top of TiO_2 layer using Physical Vapor Deposition (PVD) machine with 2nd mask (metal mask) to pattern Al contact	6 minutes
8	Preparation of polydimethylsiloxane (PDMS) as a liquid channel by:	1 hour
	(i) mixing elastomer (10) & curing agent (1)	
	(ii) baked in oven at temperature of 200°C	
	(iii) PDMS patterning using 3rd mask (plastic mold)	
9	PDMS bonding on top of ITO glass using adhesive tape	
10	Post-bake at 200°C in oven	2 hours

A top view of a liquid-based memristor sensor with nine-well structure having a diameter of 3 mm each is shown in Figure 3. Each layer of this sensor plays its own role. The TiO_2 layer with the nine-well stucture serves as the sensing layer. While the Al contact serves as the upper electrode and the ITO glass as the lower electrode. The PDMS liquid channel serves to transport liquid and become a reaction chamber.

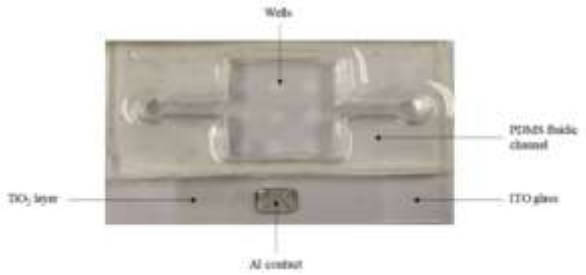

Figure 3. Top view of liquid-based memristor sensor.

2.3 Characterization

The Keithley 4200-SCS Semiconductor Characterization System is used to characterize memristor behavior in terms of current-voltage (I-V) characteristic curves. The voltage is swept from -5 V to 0 V, 0 V to 5V and 5 V to -5V. The characterization of sensor was studied in two conditions, i.e. the sensor was tested without liquid glucose and the sensor was tested with four concentrations of liquid glucose, namely 10, 20, 30, and 40 mM. These four glucose concentrations were tested on three memristor sensors that had different spin speeds for the TiO_2 sol-gel coating which were 2000, 2500, and 3000 rpm respectively.

3. RESULTS AND DISCUSSIONS

The experimental and calculation results are divided into two main parts. The first part shows the experimental and calculation results for three memristor sensors with spin speed of TiO_2 sol-gel coating of 2000, 2500 and 3000 rpm respectively. These three sensors were tested without liquid glucose.

Figure 4(a) shows the I–V characteristics of three memristor sensors (each of them has a different spin speed of TiO_2 sol-gel coating of 2000, 2500 and 3000 rpm) tested without liquid glucose. This memristor sensor behaves the same as a normal memristor. However, small changes in current were observed in each voltage sweep from 0 to 5 V for all three sensors. As spin speed of TiO_2 coating is increased, the hysteresis loop area also increased due to the decrement of the thickness of TiO_2 layer.

The R_{OFF}/R_{ON} ratio for five reading voltages of 1, 2, 3, 4 and 5 V are calculated and plotted in Figure 4(b). This graph shows that the ratio increases as the spin speed increases. This ratios changes in descending order with increasing voltage for each spin speed.

The linear graph in Figure 4(c) shows the relationship between R_{OFF}/R_{ON} ratio and spin speed at a reading voltage of 2 V. The highest ratio value of 1.27 was recorded for a spin speed of 3000 rpm followed by 1.19 recorded for a spin speed of 2500 rpm and 1.10 recorded for a spin speed of 2000 rpm.

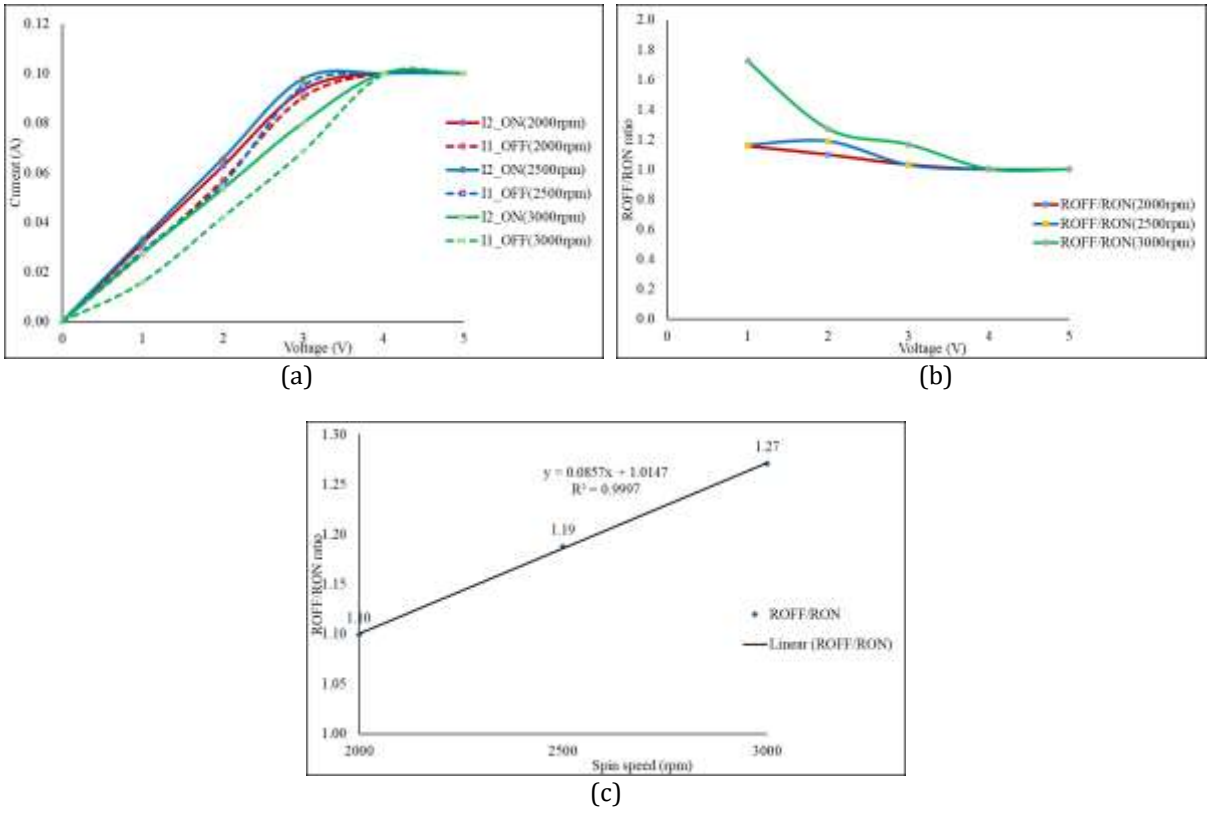

(a) (b)

(c)

Figure 4. (a) I-V characteristics of memristor sensor with a different spin speed of TiO_2 sol-gel (b) R_{OFF}/R_{ON} ratio of memristor sensor for different spin speed of TiO_2 sol-gel (c) R_{OFF}/R_{ON} ratio of memristor sensor for different spin speed at reading voltage of 2 V.

The second part shows the experimental and calculation results for three memristor sensors with spin speed of TiO_2 sol-gel coating of 2000, 2500 and 3000 rpm respectively. These three sensors were tested with four liquid glucose concentrations of 10, 20, 30, and 40 mM.

Figure 5(a) shows the I-V characteristics of memristor sensors with spin speed of TiO_2 sol-gel coating of 2000 rpm tested with different concentration of liquid glucose. It behaves like a normal memristor. Based on the graph, a small change in current was observed at each voltage sweep of 0 to 5 V when different liquid glucose concentrations were tested. By increasing the concentration of liquid glucose, the area of the hysteresis loop will also increase. The 40 mM liquid concentration the largest hysteresis loop area, followed by 30 mM, 20 mM, and 10 mM. It was found that the area of the hysteresis loop will enlarge when the concentration of liquid glucose is increased.

Figure 5(b) shows the calculated R_{OFF}/R_{ON} ratio at five reading voltages of 1, 2, 3, 4 and 5 V for a spin speed of 2000 rpm TiO_2 sol-gel coating. This graph shows the ratio is decreasing for reading voltages between 1 to 5 V. The highest ratio was recorded at a reading voltage of 1 V. The ratio increased as the glucose concentration increased .

The linear graph in Figure 5(c) shows the relationship between R_{OFF}/R_{ON} ratio and glucose concentrations at reading voltage of 2 V. The highest ratio value of 1.40 is recorded for highest glucose concentration of 40 mM. Referring to the graph, the sensitivity, *S* of the memristor sensor can be calculated using equation (3) where it is equal to 35 $(mM)^{-1}$.

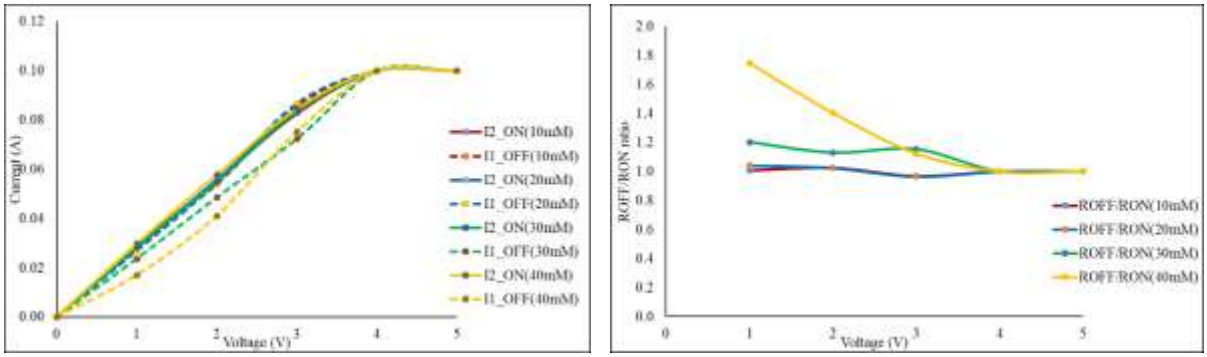

(a) (b)

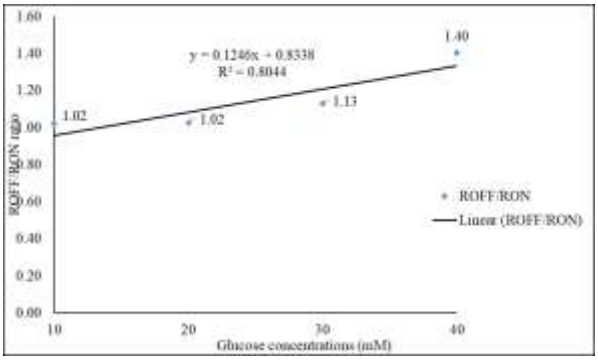

(c)

Figure 5. (a) I-V characteristics of memristor sensor with different glucose concentrations (b) R_{OFF}/R_{ON} ratio of memristor sensor for different glucose concentrations (c) R_{OFF}/R_{ON} ratio of memristor sensor for different glucose concentrations at reading voltage of 2 V.

Figure 6(a) shows the I-V characteristics of memristor sensors with spin speed of TiO_2 sol-gel coating of 2500 rpm tested with different concentration of liquid glucose. It behaves like a normal memristor. Based on the graph, a small change in current was observed at each voltage sweep of 0 to 5 V when different liquid glucose concentrations were tested. As the liquid glucose concentration is increased, the area of the hysteresis loop will also increase. The 40 mM liquid concentration the largest hysteresis loop area, followed by 30 mM, 20 mM and 10 mM. It was found that the area of the hysteresis loop will enlarge when the concentration of liquid glucose is increased.

Figure 6(b) shows the calculated R_{OFF}/R_{ON} ratio at five reading voltages of 1, 2, 3, 4 and 5 V for a spin speed of 2500 rpm TiO_2 sol-gel coating. This graph shows the ratio is decreasing for reading voltages between 1 to 5 V. The highest ratio was recorded at a reading voltage of 1 V. There are some ratio errors at reading voltages between 1 to 3 V for glucose concentrations of 10 mM and 30 mM. The ratio for 10 mM should be smaller than 20mM followed by 30 mM and 40 mM.

The linear graph in Figure 6(c) shows the relationship between R_{OFF}/R_{ON} ratio and glucose concentrations at reading voltage of 2 V. The highest ratio value of 1.42 is recorded for highest glucose concentration of 40 mM. Referring to the graph, the sensitivity, *S* of the memristor sensor can be calculated using equation (3) where it is equal to 35.5 $(mM)^{-1}$.

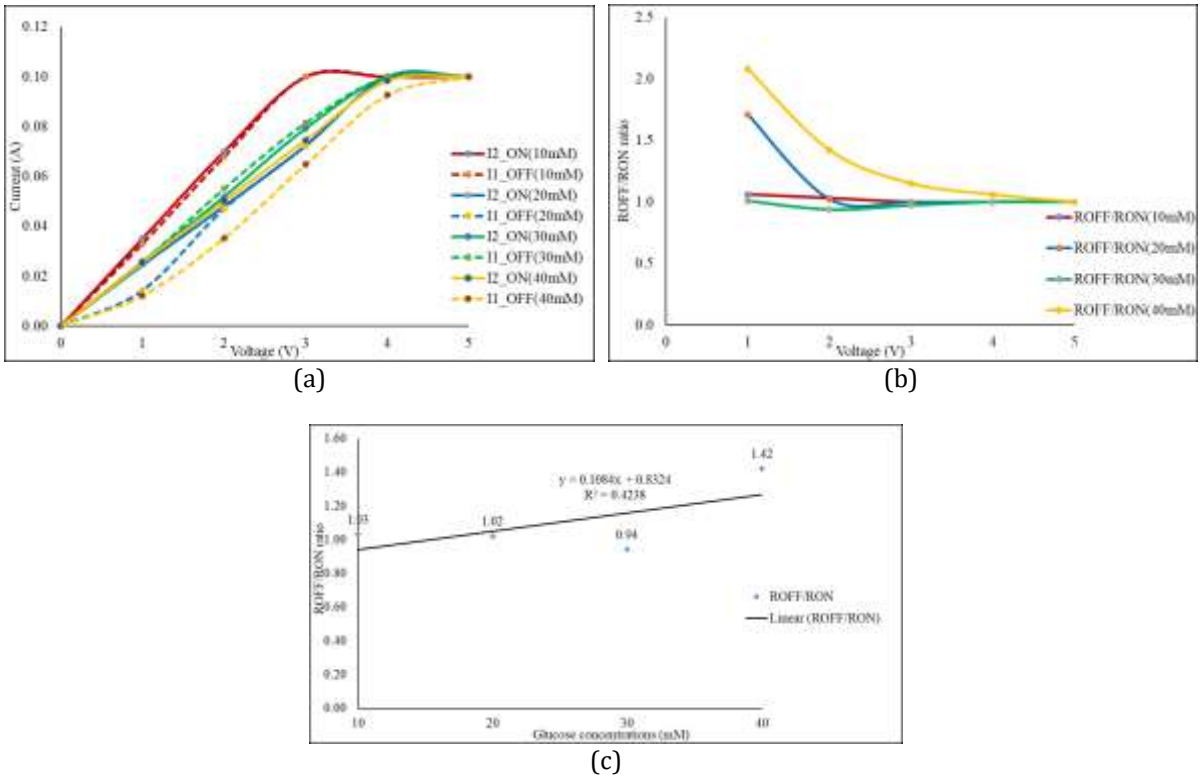

(a) (b)

(c)

Figure 6. (a) I-V characteristics of memristor sensor with different glucose concentrations (b) R_{OFF}/R_{ON} ratio of memristor sensor for different glucose concentrations (c) R_{OFF}/R_{ON} ratio of memristor sensor for different glucose concentrations at reading voltage of 2 V.

Figure 7(a) shows the I-V characteristics of memristor sensors with spin speed of TiO_2 sol-gel coating of 3000 rpm tested with different concentration of liquid glucose. It behaves like a normal memristor. The graph shows a small change in current was observed at each voltage sweep of 0 to 5 V when different liquid glucose concentrations were tested. As the liquid glucose concentration is increased, the area of the hysteresis loop will also increase. The 40 mM liquid concentration the largest hysteresis loop area, followed by 30 mM, 20 mM and 10 mM. It was found that the area of the hysteresis loop will enlarge when the concentration of liquid glucose is increased.

Figure 7(b) shows the calculated R_{OFF}/R_{ON} ratio at five reading voltages of 1, 2, 3, 4 and 5 V for a spin speed of 3000 rpm TiO_2 sol-gel coating. This graph shows the ratio is decreasing for reading voltages between 1 to 5 V. The highest ratio was recorded at a reading voltage of 1 V. The ratio also increased as the glucose concentration increased.

The linear graph in Figure 7(c) shows the relationship between R_{OFF}/R_{ON} ratio and glucose concentrations at reading voltage of 2 V. The highest ratio value of 2.25 is recorded for highest glucose concentration of 40 mM. Referring to the graph, the sensitivity, *S* of the memristor sensor can be calculated using equation (3) where it is equal to 56.25 $(mM)^{-1}$.

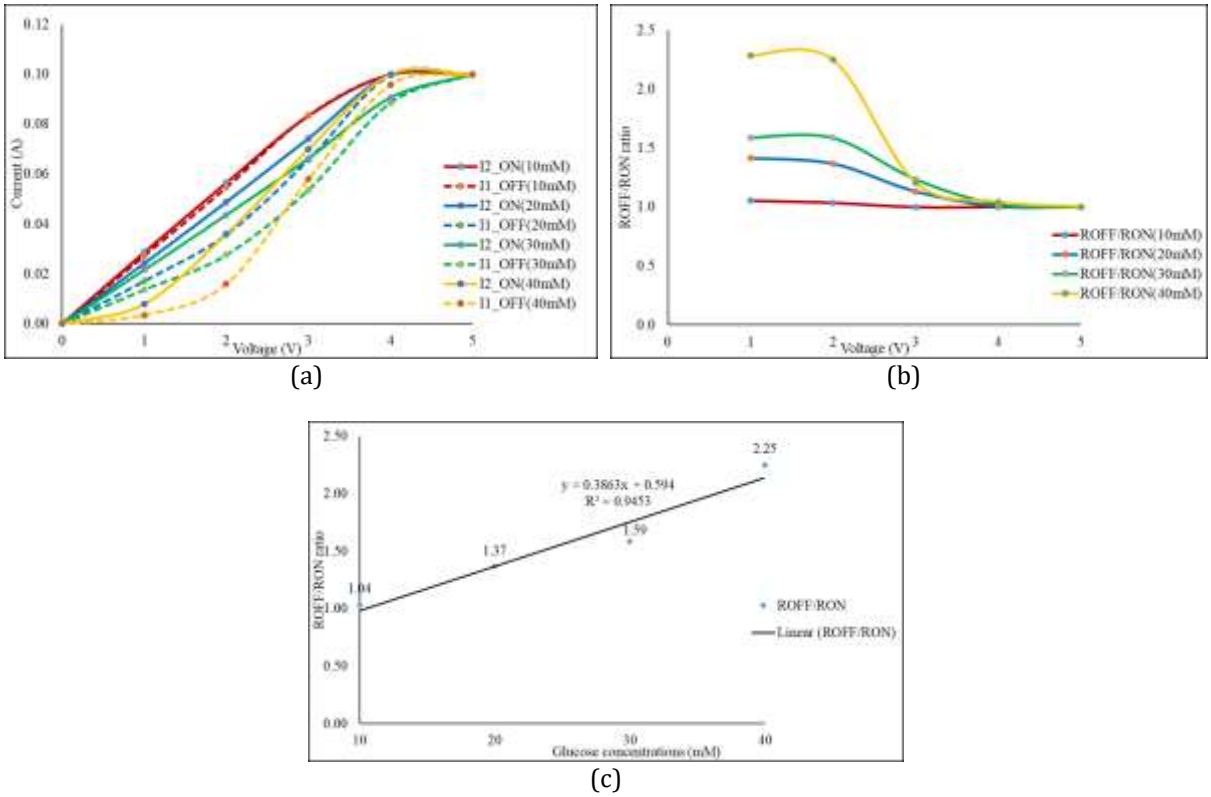

Figure 7. (a) I-V characteristics of memristor sensor with different glucose concentrations (b) R_{OFF}/R_{ON} ratio of memristor sensor for different glucose concentrations (c) R_{OFF}/R_{ON} ratio of memristor sensor for different glucose concentrations at reading voltage of 2 V.

4. CONCLUSION

The liquid-based memristor sensor with a nine-well structure have been designed and fabricated. Each well structure built on the TiO_2 layer has the same diameter of 3 mm. A large well diameter contributes to a high R_{OFF}/R_{ON} ratio. The thickness of the TiO_2 layer is different for the three sensors because it depends on the spin speed of the TiO_2 sol-gel coating which is 2000, 2500 and 3000 rpm respectively. Four glucose concentrations of 10, 20, 30, and 40 mM were prepared and tested on the three memristor sensors that having different TiO_2 thicknesses. The presence of liquid glucose, which is a hydroxide-based liquid also contributes to the change in the R_{OFF}/R_{ON} ratio. It can be concluded that there is a reaction between oxide ion, O^{2-} in TiO_2 layer and hydroxide ion, OH^- in liquid glucose. As the liquid glucose concentration increased, the ratio increased. The sensitivity of memristor sensor is directly proportional to the ratio. With the highest spin speed of 3000 rpm, the memristor sensor will have the highest ratio and in turn contributes to the high sensitivity of the sensor.

ACKNOWLEDGEMENT

First of all, I would like to express my deepest appreciation to my supervisor, Associate Prof. Dr. Asrulnizam Abd Manaf for the knowledge and guidance given. I would also like to thank Universiti Sains Malaysia and Universiti Malaysia Perlis for providing and allowing me to use research facilities in carrying out this research.

REFERENCES

[1] L. Chua, Memristor-The Missing Circuit Element, IEEE Transaction On Circuit Theory, vol. ct-18, (1971) no. 5.
[2] M. Di Ventra, Y.V Pershin, and L.O. Chua, Circuit elements with memory: memristors, memcapacitors and meminductors, no. 1, (2009) pp. 1–6.
[3] D.B. Strukov, G.S. Snider, D.R. Stewart, and R.S. Williams, The missing memristor found, Nature, vol. 453, no. 7191, (2008) pp. 80–83.
[4] Enrique Miranda and Jordi Suñé, Memristors for Neuromorphic Circuits and Artificial Intelligence Applications, Materials, (2020) 13, 938.
[5] F. Puppo, M. Di Ventra, G. De Micheli, and S. Carrara, Memristor-Based Devices for Sensing, (2014) pp. 2257–2260.
[6] I. Tzouvadaki, A. Tuoheti, S. Lorrain, M. Quadroni, M. Doucey, G. De Micheli, D. Demarchi and S. Carrara, Multi-panel, on-single-chip Memristive Biosensing, IEEE, (2018) 1558-1748 (c).
[7] N.S.M. Hadis, A.A. Manaf, M.F.A. Rahman, S.H. Ngalim, T.H. Tang, M. Citartan, A. Ismail, S.H. Herman, Fabrication and Characterization of Simple Structure Fluidic-Based Memristor for Immunosensing of NS1 Protein Application, Biosensors, (2020) 10, 143.
[8] T. Fu, X. Liu, H. Gao, J.E. Ward, X. Liu, B. Yin, Z. Wang, Y. Zhuo, D.J.F. Walker, J.J. Yang, J. Chen, D.R. Lovely & J. Yao, Bioinspired bio-voltage memristors, Nature Communications, (2020)11:1861.
[9] W.S. Zhao et al., Design and analysis of crossbar architecture based on complementary resistive switching non-volatile memory cells, J. Parallel Distrib. Comput., vol. 74, no. 6, (2014) pp. 2484–2496.
[10] Reşat Mutlu and Ertuğrul Karakulak, A Simple Test for Memristors with High ROFF/RON Ratio, European J. Eng. App. Sci. 2(1), (2019)1-5.
[11] D.S.M. Doucey, G. De Micheli, and Y. Leblebici, New Insight on Bio-sensing by Nano-fabricated Memristors, vol. 338, (2011) pp. 1–3.
[12] S. Carrara, D. Sacchetto, M. Doucey, C. Baj-rossi, G. De Micheli, and Y. Leblebici, Sensors and Actuators B: Chemical Memristive-biosensors: A new detection method by using nanofabricated memristors, Sensors Actuators B. Chem., vol. 171–172, (2012) pp. 449–457.
[13] I. Tzouvadaki, F. Puppo, M. Doucey, G. De Micheli, and S. Carrara, Modeling Memristive Biosensors, (2015) pp. 1–4.
[14] I. Tzouvadaki et al., Study on the bio-functionalization of memristive nanowires for optimum memristive biosensors, J. Mater. Chem. B, vol. 4, no. 12, (2016) pp. 2153–2162.
[15] A. Vallero et al., Memristive Biosensors Integration with Microfluidic Platform, IEEE Trans. Circuits Syst. I Regul. Pap., vol. 63, no. 12, (2016) pp. 2120–2127.
[16] I. Tzouvadaki, A. Tuoheti, G. De Micheli, D. Demarchi, and S. Carrara, Portable Memristive Biosensing System as Effective Point-of-Care Device for Cancer Diagnostics, Proc. - IEEE Int. Symp. Circuits Syst., vol. (2018).
[17] H. Duwarah and J. Devi, An approach to design memristive biosensor by using Zinc Oxide nanosample, 2019 2nd Int. Conf. Innov. Electron. Signal Process. Commun., (2019) pp. 18–22.
[18] B. Ibarlucea, T.F. Akbar, K. Kim, T. Rim, C. Baek, and A. Ascoli, Ultrasensitive detection of Ebola matrix protein in a memristor mode, vol. 11, no. 2, (2018) pp. 1057–1068.
[19] L. Chen, C. Li, T. Huang, X. Hu, and Y. Chen, The bipolar and unipolar reversible behavior on the forgetting memristor model, Neurocomputing, vol. 171, (2016) pp. 1637–1643.
[20] B. Mohammad, M.A. Jaoude, V. Kumar, D.M.A. Homouz, H.A. Nahla, M. Al-Qutayri and N. Christoforou, State of the art of metal oxide memristor devices, Nanotechnol Rev. (2016), 5(3):311–29.